Synthesis of Co, Fe co-doped SnO_2: characterization and applications

K. Chedala[a,b,c], A. Benhaoua[b], A. Hima[d,*], R. Gheriani[a,c], L. Segueni[b], L. Ayachi[b]
[a]*Faculty of Mathematics and Material Sciences, Univ. Ouargla, Ouargla 30000, Algeria*
[b]*Lab. VTRS, Faculty of Science & Technology, Univ. El-Oued, El Oued 39000, Algeria*
[c]*Lab. LRPPS, UKM Ouargla 30000, Algeria*
[d]*Department of Electrical Engineering, Fac. Technology, University of El Oued, El Oued, 39000, Algeria*

Thin films of iron and cobalt co-doped tin oxide were deposited by spray pyrolysis technique on heated glass at 480°C with moving nozzle method. The weight ratio of Fe/Co co-doped SnO_2 (Fe CTO) changed in the range of 4-16 wt.%. The structural, optical and biological characteristics were carried out by using different characterization techniques, Results from XRD, SEM, EDX and UV-Vis analyses demonstrated successful synthesis shows polycrystalline structures with cassiterite tetragonal crystal phase with a preferential orientation for co-doped SnO_2 toward (*211*), The average grain size of the thin films was found to be 39.29 nm, SEM images showed that all sample having uniform morphology with variant shape upon increasing dopant concentration, Transmittance spectra of all the thin films display high transparency more than 80% in the visible region, and band gap (E_g) varies from 3.49 to 3.75 eV. Antibacterial activity of the doped SnO_2 thin films is studied were investigated by agar method as showed good activity against both Gram-negative Escherichia coli (E.coli) and Gram-positive bacteria Staphylococcus aureus (S.aureus).confirming these as future broad-spectrum antibacterial. Thus the preparation is a good candidate for further development into therapeutic formulations.

(Received May 19, 2022; Accepted October 12, 2022)

Keywords: Thin films, Fe/Co co-doped SnO_2, Spray pyrolysis, Antibacterial activity.

1. Introduction

Transparent wide band gap semiconductors such that have versatile nature that makes them more attractive in many applications due to their excellent high transparency in the visible region of the electromagnetic spectrum. Semiconductor materials with a wide band gap offer very attractive possibilities of application, among others in electric and optoelectronic structures, Transparent conducting oxides (TCO) are widely used in microelectronic devices, light-emitting diodes, thin films, antireflection coatings, transparent electrodes in solar cells[1, 2], gas sensors surface acoustic wave devices[3], varistors, spintronic devices and lasers[4].

There is a large number of TCOs, the most commonly known ones are the binary systems, i.e. SnO_2, ZnO, In_2O_3, Ga_2O_3, and CdO[5, 6]. A large variety of ternary (Cd_2SnO_4, $CdSnO_3$, $CdIn_2$). Thin films of SnO_2 can be prepared by many techniques, such as chemical vapour deposition[7],sputtering[8], sol-gel[9], reactive evaporation[10], pulsed laser ablation[11], screen printing technique[12]. Among these, spray pyrolysis is the most convenient method because of its simplicity[13]. In the present study Fe/Co co-doped SnO_2(Fe CTO)thin films were synthesized by using spray pyrolysis technique and their characterization structural, optical and biological properties were studied[14].

Human beings have been facing different types of diseases since ancient times caused by pathogenic microbes. Among these pathogenic microbes, bacteria have a large share in spreading different infections and fatal diseases. Scientists are trying to develop various chemical agents

* Corresponding author: abdelkader-hima@univ-eloued.dz
https://doi.org/10.15251/DJNB.2022.174.1163

known as medicines for fighting against these pathogens. Therefore it is of great importance to know and to understand antimicrobial effects of the synthesized samples. A number of samples are being synthesized and their antimicrobial behavior also being studied. Different studies have shown that the concentrations ,as well as size, are the main factors that mainly control bioactivity[15].Our study focuses on enhancing these properties by doping.

This work aims to deposit 0- 16 wt% iron and cobalt co-doped tin oxide thin films on 480°C heated glass substrates using spray pyrolysis with a moving nozzle[16].Then we study their structural and optical properties upon dopant concentration.

The next is to study the antibacterial activity against Escherichia coli(E.coli) and Staphylococcus aureus (S. aureus).

2. Experimental procedure

2.1. Preparation of the spray solution

The un-doped, Fe/Co co-doped tin oxide thin films were prepared using a chemical spray pyrolysis technique with a moving nozzle (SPMN). Stannous chloride ($SnCl_2$,$2H_2O$) was used as a precursor for tin. Cobalt chloride dehydrates ($CoCl_2$, $6H_2O$) and iron chloride ($FeCl3)_a$s sources of Sn, Co, and Fe elements, respectively. The precursor was liquefied in double-distilled water and methanol (volumeratio1:1) with adding a few drops of (HCl).

The blend solutions were sprayed for 4,8,12 and 16 wt.% Fe and Co co-doped SnO_2. An R217102 microscopic glass slide in size of (75 x 25 x 1.1 mm3) was used as substrates The substrates temperature was fixed at 480°C. Whereas the deposition time was 4min with a spray rate of 5ml/min. The moving nozzle was used to save the stability of substrate temperature After deposition, the films were allowed to cool down naturally at room temperature (rt) .

2.2. Characterization

Structural properties are accomplished using an X-ray diffractometer (BRUKER-AXS type D8)Supported with X'Pert High Score working under Cu Kα (λ = 1.5405 Å) radiation and a range between 2θ=20° and 80°. Surface morphology was examined the films is by done with the scanning electron microscope (SEM).The optical properties of the deposited films were measured over the range 300–900 nm using (UV–VIS spectrophotometer Shimadzu, Model 1800). The other the optical band gap were estimated using data and fitting of The optical transmittance spectrum.

2.3. Antibacterial activity

The antibacterial activity of Fe/Co co-doped SnO_2 thin films (0-16wt.%) was studied using the agar-well diffusion method and analyzed against Gram-positive as Staphylococcus aureus, (ATCC 6538: S.a) and Gram-negative as Escherichia Coli, (ATCC 8737 : E.C) Miller Hinton agar (MHA) was poured into a sterilized Petri dish and solidified within 10min. E.coli, S. Aureus bacterial suspensions were uniformly inoculated on solidified agar gel. The sterilized samples were placed in the Petri dishes. The Petri dishes are incubated at 37°C for 24 hrs. Optical images of the plates were taken.

3. Results and discussion

3.1. Structural analysis

The crystal structure of the as-deposited Fe/Co co-doped SnO_2(FeCTO)thin films was determined by the X-ray diffraction technique. The XRD patterns obtained for the films at different ratios are studied in the 2θ range of 10 -90° as can be seen in Figure 1. six diffraction peaks were observed 2θ=26.67°, 33.344°,38.035°,51.816°,54.712°,61.886°and 65.898°,which canbe attributed respectively to the plane of (*110*), (*101*), (*200*), (*211*), (*220*), (*310*)and (*301*). The obtained XRD spectra accorded well with the space group P42mnm according to JCPDS (No. 41-1445) of the tetragonal, rutile SnO_2 structure[16].The unique feature of all the diffract grams is that they contain the characteristic SnO_2 orientations along the preferred direction (*211*). The

Appearance of other peaks as (*110*), (*101*), (*200*), (*211*), (*220*), (*310*)and (*301*) has also been detected but with substantially lower intensities. There was an increase in peak intensity (*211*) with an increase in Fe/Co co-doped doping until 8wt.% was observed which point to outgrowth in the crystallinity of the thin films shifts toward (*110*) planes. Results were shown that there is found an increase of crystallinity in the synthesized co-doped $SnO_2$when compared to the reported pure SnO_2[17]. This physical process is due to the fact that a portion of the iron and cobalt ions formed stable solid solutions with SnO_2 and ions occupy the regular lattice site in SnO_2. Thus, it may lead to the introduction of point defects and change in stoichiometry owing to charge imbalance. This results from a distortion in the crystal structure of the host compound. When the iron and cobalt ions occupy the regular lattice site in SnO_2, the interference takes place between the ions and those of SnO_2 lattice and owing to this the crystallinity of the co-doped SnO_2tends to enhance than that of pure SnO_2[18].

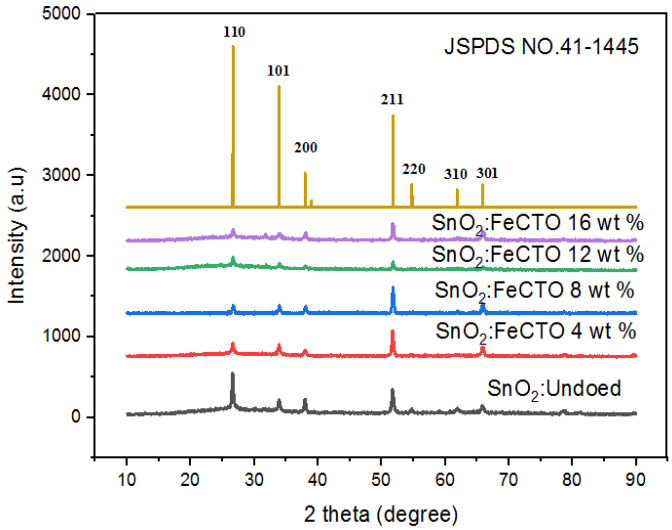

Fig. 1. XRD patterns SnO_2 images of 0-16wt.% Fe/Co co-doped SnO_2 (FeCTO) thin films.

In order to calculate the crystallite size D of Fe/Co co-doped SnO_2(FeCTO) thin films from the XRD patterns, we used Scherer's equation [19]:

$$D=\frac{0.9\lambda}{\beta \cos \theta} \quad (1)$$

where D is the crystallite size, λ is the wavelength of X-ray radiation (λ = 1.5406˚A), β is the full width at half-maximum (FWHM), and θin degrees is the half diffraction angle of the peak centroid. The values of crystallite sizes (is the position of peak) and FWHM are illustrated in Table 1. Figure 2 shows all crystallite size values as a function of doping levels. The crystallite size increases or decreases according to the ordering inside the material (density of localized states).

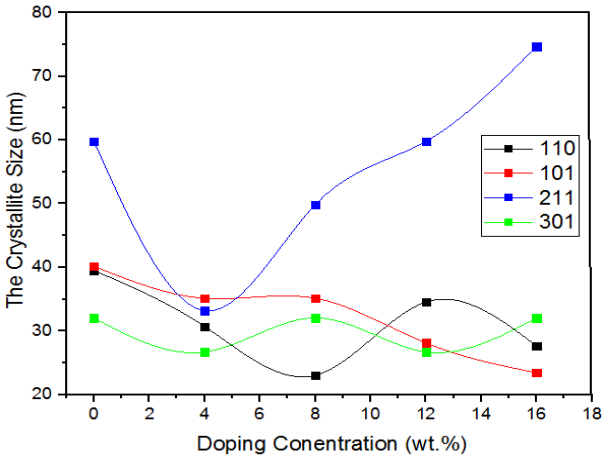

Fig. 2. The crystallite size D(nm)along different orientations for 0-16wt.% Fe/Co co-doped SnO_2 (Fe CTO) thin films.

Table 1. Average Crystallite size, Lattice Parameters and The texture coefficient TC of thin films.

FeCTO (wt.%)	Mean crystalline sizes *D* (nm)	Lattice constants (A°)				TC(hkl) of plan		
		a	$\Delta\mathbf{a} = \mathbf{a} - \mathbf{a_0}$	**c**	$\Delta\mathbf{a} = \mathbf{c} - \mathbf{c_0}$	(110)	(101)	(211)
0	46.48	4.733	-0.005	3.198	0.0109	0	0.66782	2.315242
4	31.26	4.731	-0.0072	3.188	0.0009	0.625	0.77754	2.597748
8	36.00	4.717	-0.0212	3.187	-0.0001	0.2907	0.39024	1.711219
12	40.82	4.729	-0.0092	3.172	0.0151-	0.9828	0.58187	1.427167
16	41.93	4.727	-0.0112	3.179	-0.0081	0.3547	0.33399	1.485358

The texture coefficient represents *TC* (*hkl*) the texture of the particular plane, a digression of which from unity implies the preferred growth. The different texture coefficients have been calculated from the X-ray data and lattice parameters using the following relations[20]:

$$T(hkl) = \frac{I(hkl)/I_0(hkl)}{N^{-1}\sum_n^N I(hkl)/I_0(hkl)} \quad (2)$$

and

$$\frac{1}{d_{hkl}{}^2} = \frac{h^2+k^2}{a^2} + \frac{l^2}{c^2} \quad (3)$$

where I(hkl) is then measured relative intensity of a plane (hkl), Io(hkl) is the standard intensity of the plane (hkl) taken from the JCPDS data, N is the reflection number and n is the number of diffraction peaks and ‘dhkl’ and (hkl) are the inter-planer distance and Miller indices, respectively.

The values of lattice parameters ‘a’ and ‘c’ are listed in Table1.TC (hkl) values of all the films, and with an increase in Fe and Co concentration are shown in Figure 3and recapitulated in Table1. The peaks were less than unity confirming the polycrystalline nature of the films.

It was noted that The calculated (a) values are slightly fewer than reported in the (JCPDS) card No 41-1445 (a0 = 4.737 Å); whereas, the value of the lattice constant (c)is greater than the value c0 of the JCPDS card (c0 = 3.185Å) for the doping with values at 0 and 4wt.% Fe and Co doping (FeCTO), the values of the lattice parameters (c) decreased with increasing Fe and Co doping.

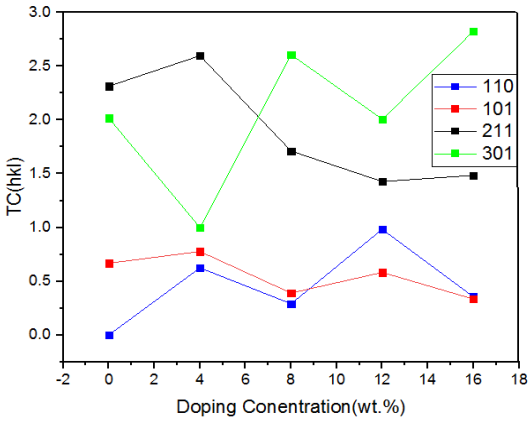

Fig. 3. TC(hkl) variation of 0-16wt.% Fe/Co co-doped SnO_2(Fe CTO) thin films.

For morphological investigation for surface, morphology is studied of as-deposited co-doped thin films (FeCTO) using field scanning electron microscopy (SEM). The SEM images of the samples were taken at 3000 × magnification. As shown in Figure 4.

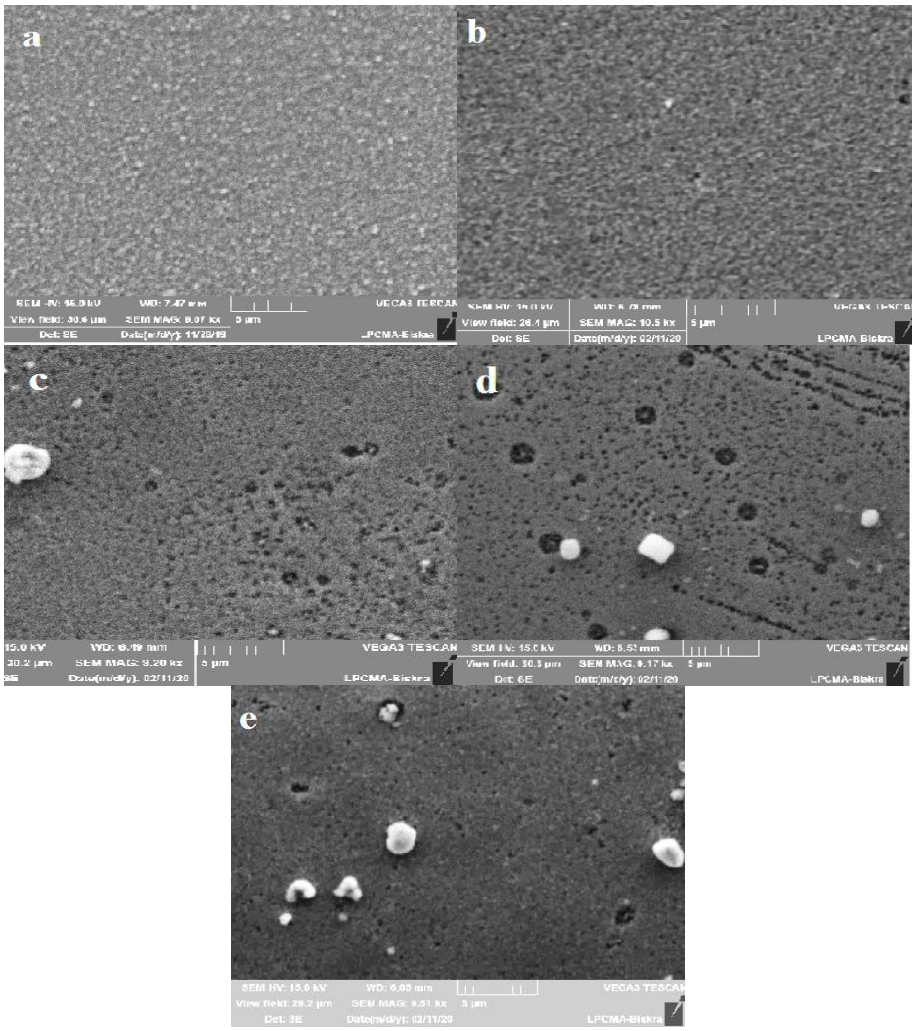

Fig. 4. SEM images of a)un-doped ,b) Fe/Co co-doped SnO_2 (Fe CTO 4wt %) c) Fe/Co co-doped SnO_2 (Fe CTO8wt %) d) Fe/Co co-doped SnO_2 (Fe CTO12wt %) e) Fe/Co co-doped SnO_2 (Fe CTO16wt %) thin films.

The un-doped sample has an homogenous surface while Fe/CO co-doped SnO_2 thin films most were present in agglomerated form The SEM investigations of synthesized co-doped reveal their crystallites nature. The same structural behavior of XRD results in terms of particles size. Moreover, Figure (b, c and d)also indicates that the synthesized co-doped agglomerations become a mixture of Fe,Co and SnO_2 had good crystalline nature. A close agreement was observed with the XRD spectra shown in Figure 1.

SEM images of the composite film surfaces showed a homogeneous distribution of the Fe/Co co-doped SnO_2 at the surface of the thin films, for every ratio and even for very high 16wt.% loadings (Figure 4). The absence of pronounced agglomerates led us to conclude a partial stabilization of the 4.wt%. interactions between the Fe,Co and SnO_2, partially replacing the surface. Indeed, Sn and O exchange between Fe and Co surfaces.

3.3. EDX analysis

EDX spectra of the un-doped and Fe/Co co-doped SnO_2thin films on glass substrates are shown in Figure 5(a) and 5(b), respectively. EDX results confirm the presence of Fe, Sn, O and Co in the grown films.

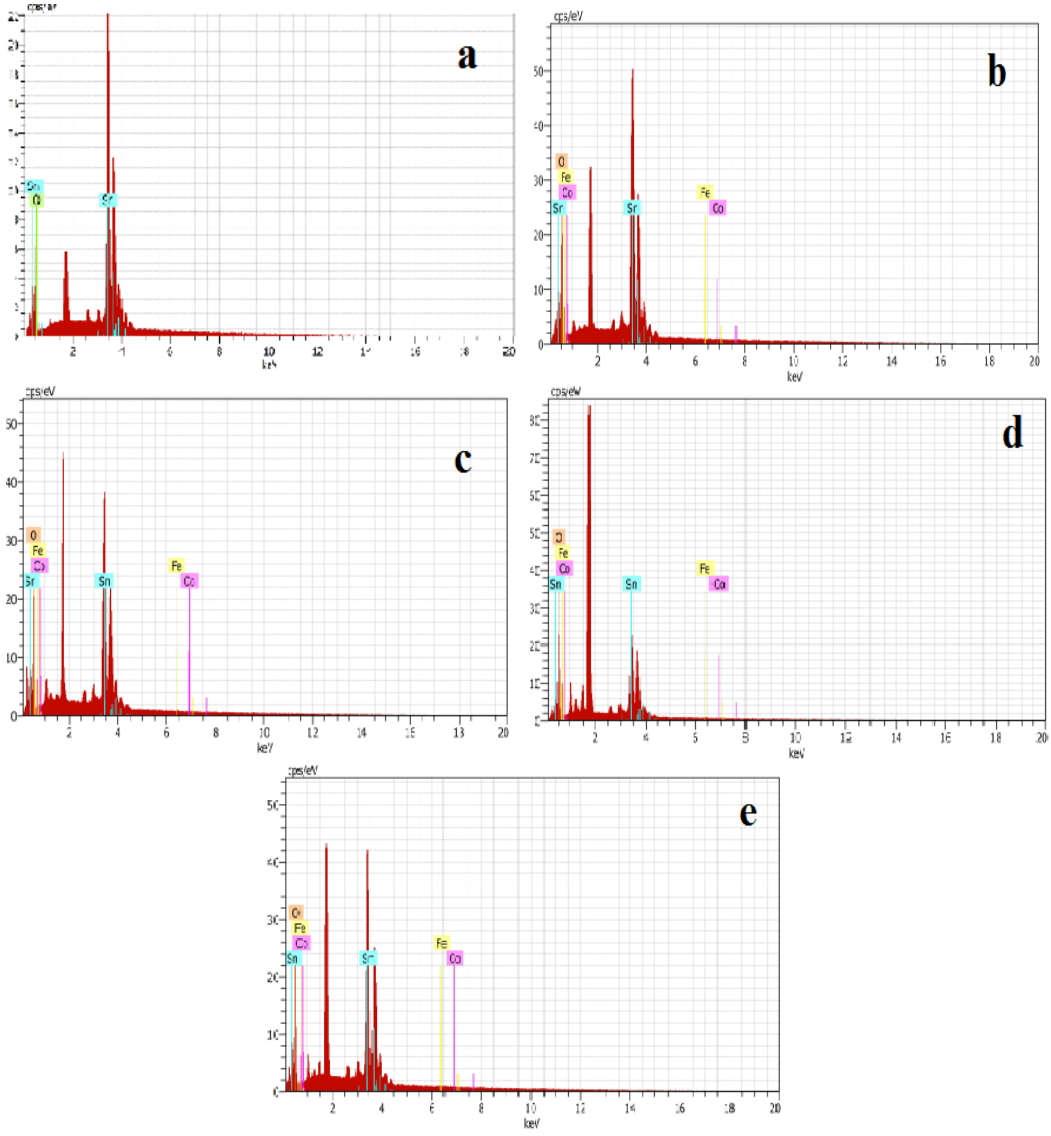

Fig. 5. EDX imagesof a) undoped ,b) Fe/Co co-doped SnO_2 (Fe CTO 4wt %) c) Fe/Co co-doped SnO_2 (Fe CTO8wt %) d) Fe/Co co-doped SnO_2 (Fe CTO12wt %) e) Fe/Co co-doped SnO_2 (Fe CTO16wt %) thin films.

The Co-doped SnO_2 are not well distributed and are present in the form of aggregates. The compositions of different Fe/Co co-dopedSnO_2 (4, 8, 12 and 16 wt. %) have been analyzed by EDX for the various elements in terms of weight %, which revealed that Fe, Co, Sn and O are present approximately as per the expected stoichiometry.

The EDX spectra taken from Fe/Co co-doped SnO_2 thin films on glass substrates are shown in Figure 5 in order to examine the chemical formation and also to confirm the presence of Fe/Co co-doped SnO_2. EDX results confirm the presence of the constituents Cobalt (Co), oxygen (O), Iron (Fe) and tin (Sn) in the grown films. The consistent and sharp peaks with tin oxide and cobalt- iron demonstrated that both synthesized were crystalline in nature [21].

Table 2. Weight (wt.%) and atomic (at.%) percentages of un-doped SnO_2 and Fe/Co co-doped SnO_2 (Fe CTO) thin films.

Composition	FeCTO 4 wt.%		FeCTO 8 wt.%		FeCTO 12wt.%		FeCTO 16wt.%	
Element	wt.%	at. %	wt.%	at.%	wt.%	at.%	wt.%	at.%
Sn	69.50	23.53	64.25	19.72	49.98	12.02	64.51	19.94
O	30.42	76.42	35.07	79.85	48.99	87.46	34.68	79.54
Fe	0.06	0.04	0.35	0.22	0.56	0.27	0.41	0.25
Co	0.01	0.01	0.33	0.21	0.47	0.24	0.40	0.26

3.4. Optical characteristics

The optical transmission measurements that have been performed are depicted by UV-vis spectroscopy is shown in Figure 6. The transmittance is greater than 80% in the visible region (400-900nm). the transmittance of the films exhibits an increase in their values after doping with Fe/Co co-doped SnO_2, reaching 98% at 12 wt.%.The results indicate that FeCTO doping can improve transmittance.

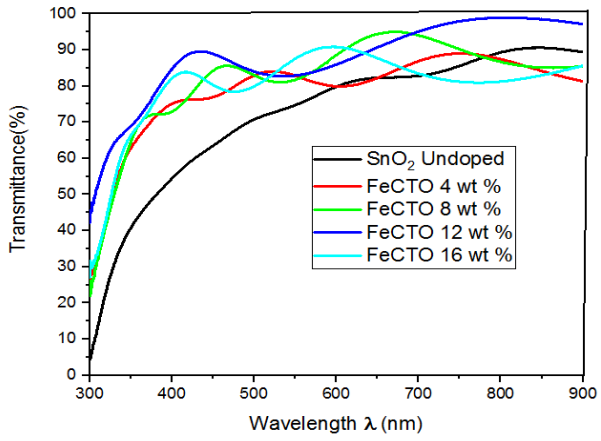

Fig. 6. Transmittance spectra of 0-16wt.% Fe/Co co-doped SnO2 (Fe CTO) thin films.

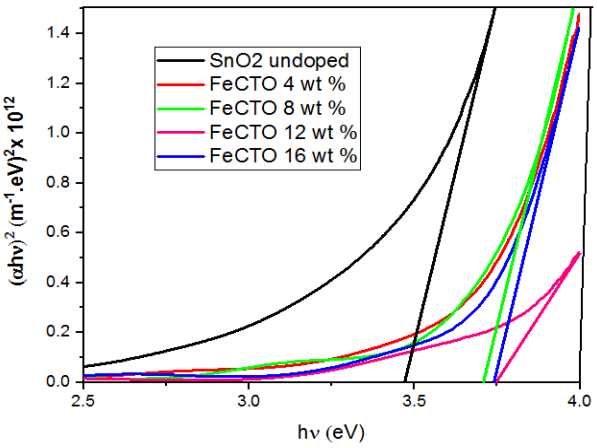

Fig. 7. Band gap (E_g) estimation from Tauc relation of 0-16wt.% Fe/Co co-doped SnO_2(Fe CTO) thin films.

Figure7 shows the variation of the optical band gap energy Eg[eV] of 0-16wt.%Fe/Co co-doped SnO_2 films, the optical band gap energy E_g[eV] was measured from the transmission spectra using Tauc's relation[22]:

$$(\mathrm{ahv})^2 = \mathrm{A}\,(\mathrm{hv} - \mathrm{Eg}) \tag{4}$$

where hv is the photon energy, α is the absorption coefficient and A is a constant, Eg is the band gap energy.

Measurement of band gap plays a vital role in semiconductors. The band gap energy of an insulator is large (> 4 eV), but is lower for a semiconductor (< 3 eV)[16]. The band gap values of co-doping thin films are increased after doping from 3.49 to 3.75 eV. This increase in the energy band gap was already observed in Co and Fe doped SnO_2[17], as well as, in other transition doped oxides. also, it may be related to the increase in the grain size which is inverted to E_g. It is clear that the optical band gap increases with the increase of FeCTO doping levels, which may be attributed to The Burstein- Moss effect[23]. That is mean the increase of the carrier density of the doped thin films and filling of states in the conduction band, which can lead to an increase in the optical band gap.

3.5. Antibacterial activity

The antibacterial activity of films was tested against the bacteria Escherichia coli(E.coli),Staphylococcus aureus (S. aureus) and the results are given in figure 8.It is clear that the synthesized SnO_2 films doped show good activity against bacteria (E.coli), (S. aureus). The antibacterial action of the prepared SnO_2 films doped increases as the concentration increases. This study confirms the use of Fe/Co co-doped SnO_2 (FeCTO) as future antibacterial[24].

All the samples of doped SnO_2 showed antibacterial activity except un-doped SnO_2. Whereas SnO_2 films doped 8, 12, 16wt.% has shown excellent antibacterial activity clearly visible against E. coli in Figure 8.

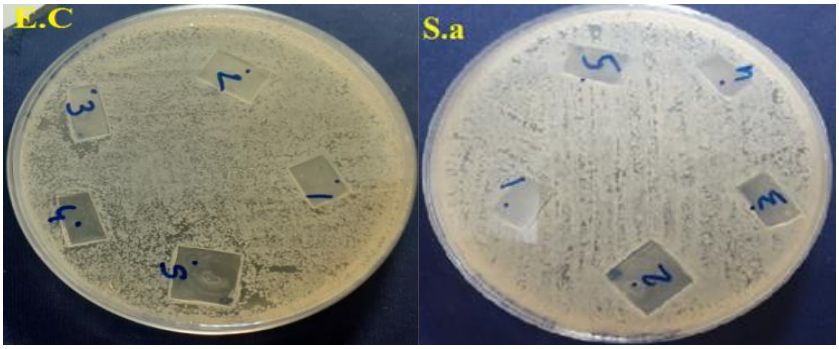

Fig. 8. Antibacterial activity of 1) un-doped ,2) Fe/Co co-doped SnO_2 (Fe CTO 4wt %) ,3) Fe/Co co-doped SnO_2 (Fe CTO8wt %), 4) Fe/Co co-doped SnO_2 (Fe CTO12wt %) ,5) Fe/Co co-doped SnO_2 (Fe CTO16wt %) against E. Coli and S.aureus.

4. Conclusion

Un-doped and Fe/Co co-doped SnO_2 thin films are successfully were prepared using spray pyrolysis method where The dopant concentration is varied at 4, 8, 12, and 16wt.%. XRD show the presence of polycrystalline structure with a tetragonal crystal structure. Both the un-doped and doped tin oxide films grow along (*211*) as preferred orientation. Whereas the grain size varies upon with increasing the dopant concentration and it was arranged in 31-46 nm. Optical transparency values increase of the films in visible spectra from 80% - 98.3%.The averaged Eg, increase from 3.49 eV to 3.75 eV with increasing the dopant concentration. The results of this study indicate that hat the synthesized Fe/Co co-doped SnO_2 thin films possess biological properties potent as doped SnO_2 thin films showed antibacterial activity against Escherichia coli (E.coli), Staphylococcus aureus (S. aureus).This was due to the fact of physical characteristics of co-doped SnO_2.Thus these synthesized hold enormous potential for use in the cosmetic, nutraceutical and pharmaceutical industries.

Acknowledgements

This research was supported in part by LPCMA Laboratory of Thin Films, University of Biskra and VTRS laboratory of Echahid Hamma Lakhdar University of El-Oued.

References

[1]C. Zhang, High-quality oriented ZnO films grown by sol-gel process assisted with ZnO seed layer, Journal of Physics and Chemistry of Solids 71, 364-369 (2010); https://doi.org/10.1016/j.jpcs.2010.01.001

[2]S. Benramache and B. Benhaoua,Influence of annealing temperature on structural and optical properties of ZnO: In thin films prepared by ultrasonic spray technique, Superlattices and Microstructures 52, 1062-1070(2012); https://doi.org/10.1016/j.spmi.2012.08.006

[3]Ü. Alver, A. Kudret, and S. Tekerek, Spray pyrolysis deposition of ZnO thin films on FTO coated substrates from zinc acetate and zinc chloride precursor solution at different growth temperatures, Journal of Physics and Chemistry of Solids 72, 701-704(2011); https://doi.org/10.1016/j.jpcs.2011.02.017

[4]P. Prepelita, R. Medianu, B. Sbarcea, F. Garoi, and M. Filipescu, The influence of using different substrates on the structural and optical characteristics of ZnO thin films, Applied surface science 256, 1807-1811(2010); https://doi.org/10.1016/j.apsusc.2009.10.011

[5]K. Chopra, S. Major, and D. Pandya, Transparent conductors-a status review, Thin solid films102, 1-46(1983); https://doi.org/10.1016/0040-6090(83)90256-0

[6]T. J. Coutts, D. L. Young, and X. Li, Characterization of transparent conducting oxides, Mrs

Bulletin 25, 58-65(2000); https://doi.org/10.1557/mrs2000.152

[7]J. Berry, D. Ginley, and P. E. Burrows, Organic light emitting diodes using a Ga: ZnO anode, Applied Physics Letters92, 170(2008); https://doi.org/10.1063/1.2917565

[8]S. Boycheva, A. K. Sytchkova, M. L. Grilli, A. Piegari, Thin Solid Films 515(24), 8469 (2007).

[9]M.-M. Bagheri-Mohagheghi and M. Shokooh-Saremi, The influence of Al doping on the electrical, optical and structural properties of SnO2 transparent conducting films deposited by the spray pyrolysis technique, Journal of Physics D: Applied Physics 37, 1248(2004); https://doi.org/10.1088/0022-3727/37/8/014

[10]K. Omura, P. Veluchamy, M. Tsuji, T. Nishio, and M. Murozono, A pyrosol technique to deposit highly transparent, low-resistance SnO2: F Thin films from dimethyltin dichloride, Journal of the electrochemical society 146, 2113(1999); https://doi.org/10.1149/1.1391900

[11]A. Banerjee, R. Maity, P. Ghosh, and K. Chattopadhyay,Thermoelectric properties and electrical characteristics of sputter-deposited p-CuAlO2 thin films, Thin Solid Films 474, 261-266(2005); https://doi.org/10.1016/j.tsf.2004.08.117

[12]E. Fortunato, D. Ginley, H. Hosono, and D. C. Paine, Transparent conducting oxides for photovoltaics, MRS bulletin32, 242-247(2007); https://doi.org/10.1557/mrs2007.29

[13]A. Benhaoua, A. Rahal, B. Benhaoua, and M. Jlassi, Effect of fluorine doping on the structural, optical and electrical properties of SnO2 thin films prepared by spray ultrasonic, Superlattices and Microstructures70, 61-69(2014); https://doi.org/10.1016/j.spmi.2014.02.005

[14]S. A. Khan, M. Jameel, S. Kanwal, and S. Shahid, Medicinal importance of Allium species: a current review International Journal of Pharmaceutical Science and Research2, 29-39(2017).

[15]F. Ijaz, S. Shahid, S. A. Khan, W. Ahmad, and S. Zaman, Green synthesis of copper oxide nanoparticles using Abutilon indicum leaf extract: Antimicrobial, antioxidant and photocatalytic dye degradation activitie, Tropical Journal of Pharmaceutical Research 16, 743-753(2017); https://doi.org/10.4314/tjpr.v16i4.2

[16]M. Batzill and U. Diebold, "The surface and materials science of tin oxide," Progress in surface science79, 47-154(2005); https://doi.org/10.1016/j.progsurf.2005.09.002

[17]S. Khan, F. Noreen, S. Kanwal, and G. Hussain, Comparative synthesis, characterization of Cu-doped ZnO nanoparticles and their antioxidant, antibacterial, antifungal and photocatalytic dye degradation activities, Dig J Nanomater Biostruct 12, 877-89(2017).

[18]K. Anandan and V. Rajendran, Size controlled synthesis of SnO2 nanoparticles: facile solvothermal process, J. Non-Oxide Glasses 2, 83-89(2010).

[19]S. Rani, P. Suri, P. Shishodia, and R. Mehra, Synthesis of nanocrystalline ZnO powder via sol-gel route for dye-sensitized solar cells, Solar Energy Materials and Solar Cells 92, 1639-1645(2008); https://doi.org/10.1016/j.solmat.2008.07.015

[20]C. Barret and T. Massalski, Structure of Metals Pergamon Press, Oxford(1980).

[21]M. Qamar, S. Shahid, S. Khan, S. Zaman, and M. Sarwar, Synthesis characterization, optical and antibacterial studies of Co-doped SnO2 nanoparticles, Dig J Nanomater Biostruct 12, 1127-35(2017).

[22]D. M. Mattox, Handbook of physical vapor deposition (PVD) processing: William Andrew(2010); https://doi.org/10.1016/B978-0-8155-2037-5.00008-3

[23]P. V. Kamat, N. M. Dimitrijevic, and A. J. Nozik, Dynamic Burstein-Moss shift in semiconductor colloids, The Journal of Physical Chemistry93, 2873-2875(1989); https://doi.org/10.1021/j100345a003

[24]S. A. Khan, F. Noreen, S. Kanwal, A. Iqbal, and G. Hussain, Green synthesis of ZnO and Cu-doped ZnO nanoparticles from leaf extracts of Abutilon indicum, Clerodendrum infortunatum, Clerodendrum inerme and investigation of their biological and photocatalytic activities, Materials Science and Engineering: C82, 46-59(2018); https://doi.org/10.1016/j.msec.2017.08.071